

Novel phase of beryllium fluoride at high pressure

Maksim S. Rakitin,^{1,*} Artem R. Oganov,^{2,1,3,4} Haiyang Niu,^{3,5} M. Mahdi Davari Esfahani,¹ Xiang-Feng Zhou,¹ Guang-Rui Qian,¹ and Vladimir L. Solozhenko⁶

¹Department of Geosciences, State University of New York, Stony Brook, NY 11794, USA

²Skolkovo Institute of Science and Technology, Skolkovo Innovation Center, Bldg. 3, Moscow 143026, Russia

³Moscow Institution of Physics and Technology, 9 Institutskiy Lane, Dolgoprudny City, Moscow Region 141700, Russia

⁴School of Materials Science, Northwestern Polytechnical University, Xi'an 710072, China

⁵Shenyang National Laboratory for Materials Science, Institute of Metal Research, Chinese Academy of Sciences, Shenyang 110016, China

⁶LSPM-CNRS, Université Paris Nord, 93430 Villetaneuse, France

(Dated: August 30, 2018)

A previously unknown thermodynamically stable high-pressure phase of BeF₂ has been predicted using the evolutionary algorithm USPEX. This phase occurs in the pressure range 18–27 GPa. Its structure has *C2/c* space group symmetry and contains 18 atoms in the primitive unit cell. Given the analogy between BeF₂ and SiO₂, silica phases have been investigated as well, but the new phase has not been observed to be thermodynamically stable for this system. However, it is found to be metastable and to have comparable energy to the known metastable phases of SiO₂, suggesting a possibility of its synthesis.

PACS numbers:

I. INTRODUCTION

Beryllium fluoride has many applications, such as coolant component in molten salt nuclear reactors^{1,2}, production of special glasses^{3,4}, manufacture of pure beryllium⁵, etc. Structurally, BeF₂ phases are similar to the phases of SiO₂ (Fig. 1): α -quartz phase of BeF₂ and SiO₂ is stable from 0 to \sim 2 GPa, and then transforms to coesite phase which persists up to \sim 8 GPa, and then transforms to stishovite (rutile-type phase) in SiO₂⁶. However, the behavior of BeF₂ experimentally is not known for pressures above 8 GPa (see Scheme 1 in Ref.⁷).

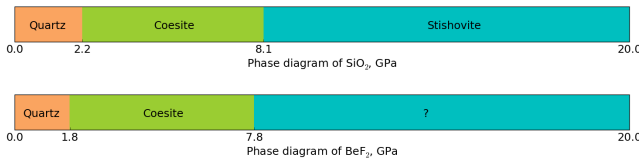


FIG. 1. Phase diagrams of SiO₂⁶ and BeF₂⁷ at low (up to room) temperatures.

One of our goals in present paper is to reveal which phase transitions can occur at higher pressures in BeF₂. Beryllium compounds are extremely toxic for humans, and this limits experimentation. Computer simulation is a safe and cheap alternative to investigate such structures. In recent *ab initio* study⁸ authors explored 13 well-known AB₂ structure types for their possible stability for BeF₂: α -quartz-type (*P3₁21*), β -quartz-type (*P6₂22*), α -cristobalite-type (*P4₁2₁2*), β -cristobalite-type (*Fd-3m*), cubic CaF₂-type (*Fm-3m*), α -PbCl₂-type (*Pnma*), Ni₂In-type (*P6₃/mmc*), coesite-type (*C2/c*), rutile-type (*P4₂/mnm*), baddeleyite-type (*P2₁/c*), α -

PbO₂-type (*Pbcn*), α -CaCl₂-type (*Pnmm*) and pyrite-type (*Pa-3*) structures. They found that the sequence of pressure-induced phase transitions of BeF₂ up to 50 GPa is as follows: α -quartz-type $\xrightarrow{0.59 \text{ GPa}}$ coesite-type $\xrightarrow{6.47 \text{ GPa}}$ rutile-type $\xrightarrow{24.94 \text{ GPa}}$ α -PbO₂-type structures. Although BeF₂ under pressure has been theoretically investigated by Yu *et al.*⁸, we revisit these results to check for previously unknown structure(s), and we explore the relevance of these findings for SiO₂.

II. COMPUTATIONAL DETAILS

Computer simulations of BeF₂ and SiO₂ has been performed in two steps: (1) prediction of a new structure of BeF₂ using USPEX evolutionary algorithm; (2) calculation of properties of BeF₂ and SiO₂ in the wide range of pressures from 0 to 50 GPa with a 1 GPa step using DFT.

To find stable lowest-energy crystals structures, we performed fixed-composition search of the BeF₂ system at different pressures (15, 20 and 25 GPa) using the USPEX code^{9–11}, in conjunction with first-principles structure relaxations using density functional theory (DFT) within the Perdew-Burke-Ernzerhof (PBE) generalized gradient approximation (GGA)¹², as implemented in the VASP package¹³. We employed projector augmented wave (PAW)¹⁴ potentials with 2 valence electrons for Be and 7 — for F. The wave functions were expanded in a plane-wave basis set with the kinetic energy cutoff of 600 eV and Γ -centered meshes for Brillouin zone sampling with reciprocal space resolution of $2\pi \times 0.10 \text{ \AA}^{-1}$.

We used the VASP package to carefully reoptimize the obtained structures before calculating phonons, elasticity, electronic density of states (DOS), hardness of

BeF₂ and SiO₂. For these relaxations, we also used the plane-wave cutoff of 600 eV and k -meshes with resolution of 0.10 Å⁻¹. Phonons calculations have been performed using Phonopy¹⁵ and Quantum Espresso¹⁶ codes for the relaxed structures at pressures where these structures are found to be thermodynamically stable. Hardness was calculated using 3 methods: Lyakhov-Oganov model¹⁷ based on the strength of bonds between atoms and bond network topology, Chen-Niu model¹⁸ which uses elastic constants obtained from DFT calculations and Mukhanov-Kurakevych-Solozhenko thermodynamic model of hardness¹⁹.

III. RESULTS AND DISCUSSION

USPEX allowed us to find a new structure of BeF₂, stable at 18–27 GPa (Fig. 2). The structure has $C2/c$ space group and contains 12 formula units in the Bravais cell (6 in the primitive cell) with $a=8.742$ Å, $b=8.695$ Å, $c=4.178$ Å and $\beta=66.1^\circ$ (at 20 GPa). Calculated density of this new $C2/c$ phase is 4.2% higher than density of coesite phase, both at 20 GPa. For reference, here are lattice parameters for BeF₂-stishovite at 30 GPa: $a=b=3.986$ Å, $c=2.501$ Å and $\alpha=\beta=\gamma=90^\circ$. The value of the bulk modulus $B_0=22.4$ GPa of the $C2/c$ structure of BeF₂ with its pressure derivative $B'_0=3.9$ was obtained from a least-squares fit using the Murnaghan equation of state²⁰ (Fig. 3). The zero-pressure unit cell volume was taken as $V_0=213.7$ Å³.

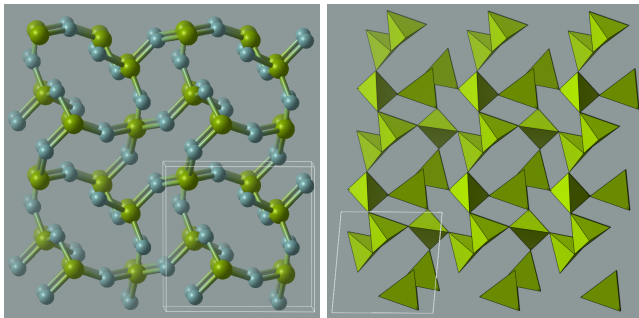


FIG. 2. $C2/c$ structure of BeF₂, stable at 18–27 GPa.

A. Thermodynamic stability

We have calculated the enthalpies of α -quartz ($P3_221$), coesite ($C2/c$), coesite-II ($C2/c$), stishovite ($P4_2/mnm$), α -PbO₂-type ($Pbcn$) structure and our new structure ($C2/c$) for both BeF₂ and SiO₂ at different pressures from 0 to 50 GPa with a 1 GPa step. The results are presented in Fig. 4.

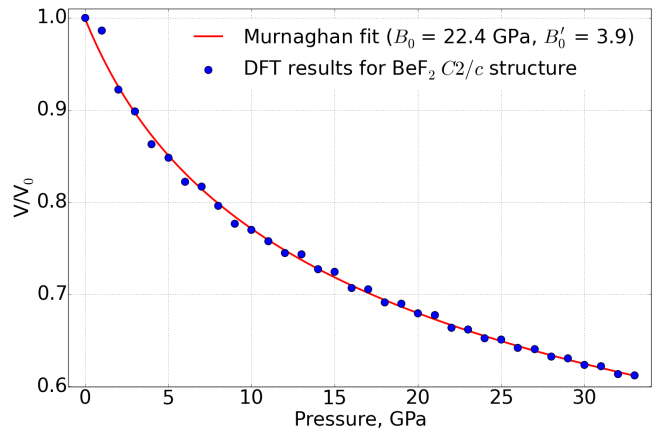


FIG. 3. Equation of state of BeF₂ $C2/c$ structure.

1. BeF₂ under pressure

For the case of BeF₂ α -quartz structure is stable from 0 to 4 GPa, followed by coesite structure stable from 4 to 18 GPa, and the $C2/c$ structure is found to be stable between 18 and 27 GPa, which then gives place to stishovite structure at higher pressures (Fig. 4(a)). We see transition from coesite-type to $C2/c$, then to rutile-type, but at much higher pressure (27 GPa against 6.47 GPa in Ref.⁸, where LDA was used). According to Demuth *et al.*²¹, the LDA approximation used in Ref.⁸ underestimates phase transition pressures, whereas using the GGA yields more reliable results. The α -PbO₂-type structure is not stable at any pressure (in the investigated interval from 0 to 50 GPa) for BeF₂ (though it is close to stability at ~ 27 GPa), while for SiO₂ it is indeed stable at pressures above ~ 80 –90 GPa²².

2. SiO₂ under pressure

From Fig. 4(b) it is clearly seen that in SiO₂ the transition from α -quartz to coesite occurs at 5 GPa, followed by transformation to stishovite at ~ 7 GPa, which continues to be stable up to 50 GPa. This phase transition sequence is in good agreement with experiments⁶ and with the GGA results by Demuth *et al.*²¹, Oganov *et al.*²² and LDA results of Tsuchiya *et al.*²³; it is known though²¹ that the GGA is more accurate than the LDA for phase transition pressures. The new structure is not stable at any pressure for SiO₂, but at 0 GPa is only 3.4 meV/atom higher in energy than α -quartz, and should be synthesizable as a metastable phase. Our results of coesite \rightarrow coesite-II transition are in good agreement with recent study of Černok *et al.*²⁴, where they observe coesite at 20.3 GPa, and after an abrupt change in the diffraction pattern between ~ 20 and ~ 28 GPa — coesite-II at 27.5 and 30.9 GPa.

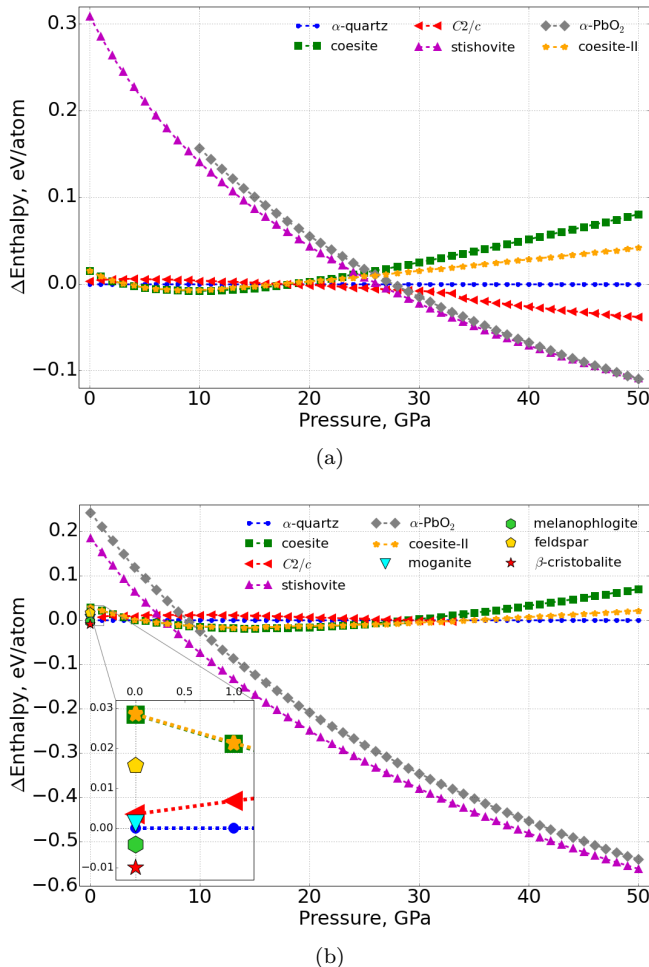


FIG. 4. Enthalpies (relative to α -quartz) of (a) BeF_2 and (b) SiO_2 phases as a function of pressure.

3. Metastable structures of SiO_2

It is well known that SiO_2 α -quartz is thermodynamically stable at ambient pressure. However, there are numerous known SiO_2 polymorphs which are metastable, but exist in nature or can be synthesized. We examined SiO_2 feldspar, baddeleyite, melanophlogite and moganite at 0 GPa. El Goresy *et al.*²⁵ claimed a baddeleyite-like post-stishovite phase of silica in the Shergotty meteorite, however later that controversial phase turned out to be α - PbO_2 -like silica²⁶. Our calculations confirm that the baddeleyite-like form of SiO_2 is very unfavorable at 0 GPa and spontaneously (barrierlessly) transforms into the α - PbO_2 -like structure. We have found that SiO_2 -feldspar, moganite and melanophlogite are energetically very close to the stable phase (α -quartz) and to the new $C2/c$ structure. Differences in enthalpy between melanophlogite, new structure and α -quartz are less than 0.01 eV/atom (see zoomed inset in Fig. 4(b)). The fact that complex open structure of melanophlogite (138 atoms/cell) has a slightly lower energy than α -

quartz, can be explained by errors of the GGA, which were discussed in details by Demuth *et al.*²¹. They also found β -cristobalite (Fig. 4(b)) is lower in energy by about 0.03 eV/ SiO_2 than α -quartz, confirmed by calculations of Zhang *et al.*²⁷, showing that the GGA slightly overstabilizes low-density structures.

B. Lattice dynamics

Since the new structure of BeF_2 appears to be thermodynamically stable, analysis of dynamical stability (phonon dispersion) has been performed for this structure as well as for all other structures at pressures where they were found to be thermodynamically stable. Our results show that BeF_2 α -quartz at 0 GPa, coesite at 5 GPa, new structure at 25 GPa and stishovite at 30 GPa do not have imaginary frequencies. Similar results are observed for SiO_2 α -quartz at 0 GPa, coesite at 5 GPa and stishovite at 10 GPa. Fig. 5 shows dynamical stability of the new structure of BeF_2 since no imaginary frequencies are observed in the phonon dispersion plot.

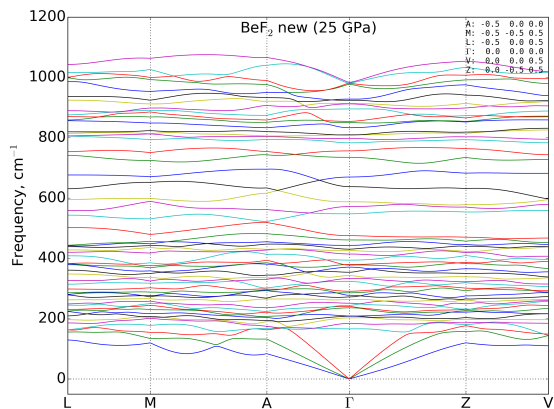


FIG. 5. Phonons dispersion curves showing dynamical stability of the $C2/c$ structure of BeF_2 at 25 GPa.

C. Electronic properties

According to Fig. 6, all BeF_2 phases are insulators, the DFT band gap increases from ~ 7 to ~ 10 eV with increasing pressure from 0 to 30 GPa and the value of the gap is in good agreement with data of Yu *et al.*⁸.

For SiO_2 (Fig. 7) we also observe insulating behavior, and the band gap is about 6 eV and remains almost unchanged with increasing pressure.

D. Hardness

Three models have been exploited to calculate hardnesses — the Lyakhov-Oganov¹⁷, Chen-Niu¹⁸ and

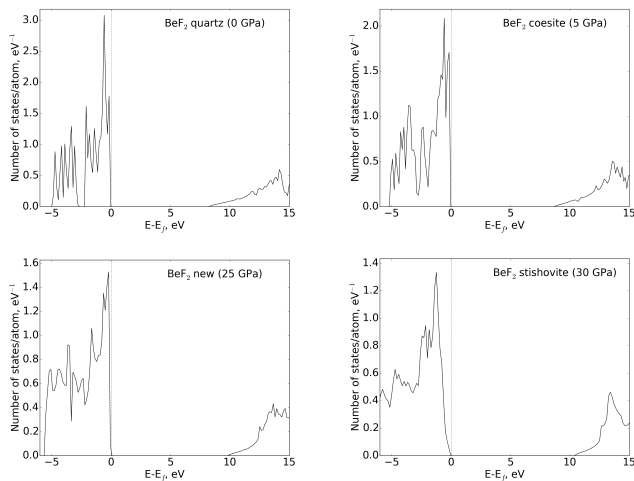
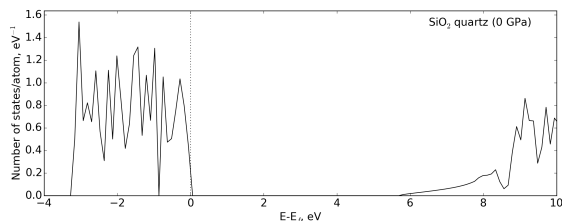
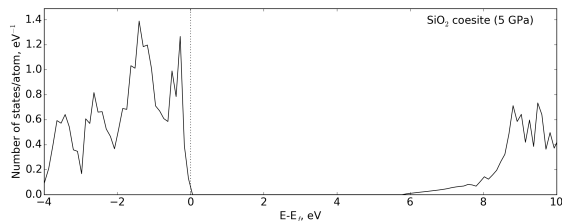


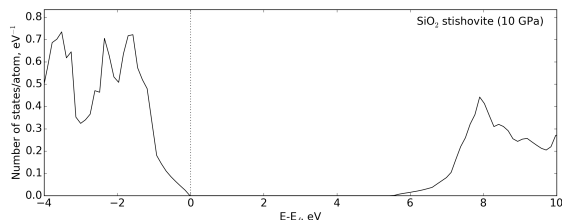
FIG. 6. Density of states of BeF_2 in the α -quartz (at 0 GPa), coesite (at 5 GPa), $C2/c$ structure (at 25 GPa), and stishovite (at 30 GPa) phases.



(a)



(b)



(c)

FIG. 7. Density of states of SiO_2 in the (a) α -quartz (at 0 GPa), (b) coesite (at 5 GPa) and (c) stishovite (at 10 GPa) phases.

Mukhanov-Kurakevych-Solozhenko¹⁹ models. First approach is based on concepts of bond strengths and bond topology to compute hardness. Detailed description of the methodology can be found in Ref.¹⁷. This model has been implemented in the USPEX code, and for greater convenience has also been implemented as an online utility available at <http://han.ess.sunysb.edu/hardness/>. The second method of hardness calculation is Chen-Niu model, which is based on elastic tensor components and also implemented in the USPEX code. The third one is a thermodynamic model of hardness.

The results can be seen in Table I. Experimental data are provided where available — Vickers hardness of SiO_2 -quartz²⁸, SiO_2 -coesite¹⁹ and SiO_2 -stishovite²⁹. From Table I it is clearly seen that the calculated hardness of SiO_2 quartz and stishovite is much higher than one of BeF_2 analogs. The hardness of BeF_2 and SiO_2 in the new $C2/c$ structure is comparable with the hardness of α -quartz and coesite.

IV. CONCLUSIONS

We have examined thermodynamic, vibrational, electronic and elastic properties of BeF_2 and SiO_2 phases using DFT calculations. The sequence of pressure-induced phase transitions of BeF_2 up to 50 GPa is as follows: α -quartz-type $\xrightarrow{4 \text{ GPa}}$ coesite-type $\xrightarrow{18 \text{ GPa}}$ $C2/c$ $\xrightarrow{27 \text{ GPa}}$ stishovite (rutile-type) structures. We found a new phase of BeF_2 which is thermodynamically stable at pressures from 18 to 27 GPa. This phase is not observed in SiO_2 , but could be synthesized in principle. Electronic properties analysis has shown BeF_2 and SiO_2 remain insulating in a wide range of pressures (from 0 to 50 GPa). Hardness of BeF_2 and SiO_2 in the new structure is comparable with hardness of α -quartz and coesite at 0 GPa. Hardnesses of metastable SiO_2 structures have been examined as well.

V. AUTHOR CONTRIBUTIONS

M.R., H.N. and M.D. performed the calculations, M.R. and A.R.O. contributed to the analysis and wrote the paper. X.F.Z and G.R.Q. provided technical assistance with calculations. V.L.S. proposed the idea, performed calculations of hardness and participated in the discussion.

VI. ADDITIONAL INFORMATION

Competing financial interests: The authors declare no competing financial interests.

TABLE I. Hardness of BeF₂ and SiO₂ structures at 0 GPa in GPa. For the metastable SiO₂ structures we present enthalpies relative to α -quartz (in eV per formula unit).

	BeF ₂			SiO ₂		
	Lyakhov-Oganov	Chen-Niu	Mukhanov <i>et al.</i> ^a	Lyakhov-Oganov	Chen-Niu	Experiment
Quartz	7.1	7.5	11.0	20.0	12.5	12.0 ^b
Coesite	8.2	8.3	11.7	22.3	8.4	20.0 ^b
New structure	7.3	6.8	13.5	19.1	6.7	—
Stishovite	8.2	12.7	15.1	29.0	28.7	33.0 ^b

Metastable structures (SiO ₂ only):			
	Relative enthalpy, eV/f.u.	Hardness, GPa	
		Lyakhov-Oganov model	Chen-Niu model
Feldspar	0.047	6.7	11.8
Baddeleyite	0.726	29.6	28.0
Melanophlogite	-0.013	12.5	3.3
Moganite	0.003	19.5	12.8

^a Thermodynamic model of hardness (Ref.¹⁹)

^b Vickers hardness

ACKNOWLEDGMENTS

We thank the National Science Foundation (EAR-1114313, DMR-1231586), DARPA (Grant No. W31P4Q1210008), the Government of Russian Federation (grant No. 14.A12.31.0003), and Foreign Talents Introduction and Academic Exchange Program (No. B08040). Also, we thank Dr. V.A. Mukhanov for valuable comments.

Appendix A: Densities of BeF₂ and SiO₂ structures

Table II shows densities of BeF₂ structures at 0 and 20 GPa and SiO₂ structures at 0 GPa.

TABLE II. Densities of BeF₂ and SiO₂ structures.

System	Number of atoms	Volume, Å ³ /cell	Density, g/cm ³
BeF₂ at 0 GPa:			
α -quartz	9	105.167	2.244
coesite	24	254.636	2.472
coesite-II	96	1021.960	2.464
<i>C2/c</i>	18	213.696	2.209
stishovite	6	47.771	3.294
BeF₂ at 20 GPa:			
α -quartz	9	73.078	3.230
coesite	24	202.001	3.116
<i>C2/c</i>	18	145.159	3.252
stishovite	6	41.492	3.793
SiO₂ at 0 GPa:			
α -quartz	9	116.934	2.580
coesite	24	283.341	2.839
coesite-II	96	1137.296	2.830
<i>C2/c</i>	18	243.569	2.477
stishovite	6	48.185	4.174
α -PbO ₂ -type	12	94.623	4.251

Appendix B: CIF file of BeF₂ *C2/c* structure at 20 GPa

```
# CIF file
# This file was generated by FINDSYM (H.T. Stokes)

data_findsym-output

_symmetry_space_group_name_H-M 'C 1 2/c 1'
_symmetry_Int_Tables_number 15

_cell_length_a      8.74241
_cell_length_b      8.69478
_cell_length_c      4.17800
_cell_angle_alpha   90.00000
_cell_angle_beta    66.07927
_cell_angle_gamma   90.00000

loop_
_space_group_symop_operation_xyz
x,y,z
-x,y,-z+1/2
-x,-y,-z
x,-y,z+1/2
x+1/2,y+1/2,z
-x+1/2,y+1/2,-z+1/2
-x+1/2,-y+1/2,-z
x+1/2,-y+1/2,z+1/2

loop_
_atom_site_label
_atom_site_type_symbol
_atom_site_fract_x
_atom_site_fract_y
_atom_site_fract_z
_atom_site_occupancy
Be1 Be  0.30175  0.08755  0.27471  1.00000
Be2 Be  0.00000  0.18404  0.25000  1.00000
F1  F  -0.11350  0.09592  0.11433  1.00000
F2  F   0.14707  0.43232  0.42082  1.00000
F3  F  -0.11681  0.27080 -0.42582  1.00000
```

- * Correspondence and requests for materials should be addressed to M.S. Rakinin (maksim.rakinin@stonybrook.edu) or A.R. Oganov (artem.oganov@stonybrook.edu)
- ¹ C. Weaver, R. Thoma, H. Insley, H. Friedman, and U. A. E. Commission, *Phase equilibria in molten salt breeder reactor fuels: The system LiF-BeF₂-UF₄-ThF₄* (Oak Ridge National Laboratory, 1961).
- ² O. Beneš and R. Konings, *Journal of Fluorine Chemistry* **130**, 22 (2009).
- ³ J. Parker and P. France, in *Glasses and Glass-Ceramics*, edited by M. Lewis (Springer Netherlands, 1989) pp. 156–202.
- ⁴ F. Gan, *Journal of Non-Crystalline Solids* **184**, 9 (1995).
- ⁵ H. Hausner, *Beryllium, its metallurgy and properties*, edited by Henry H. Hausner (University of California Press Berkeley, 1965) p. 322.
- ⁶ V. Swamy, S. Saxena, B. Sundman, and J. Zhang, *Journal of Geophysical Research: Solid Earth* **99**, 11787 (1994).
- ⁷ P. Ghalsasi and P. Ghalsasi, *Inorganic Chemistry* **50**, 86 (2011).
- ⁸ F. Yu, M. Xu, M. Jiang, and J.-X. Sun, *Solid State Communications* **169**, 14 (2013).
- ⁹ A. Oganov and C. Glass, *The Journal of Chemical Physics* **124**, 244704 (2006).
- ¹⁰ A. Oganov, A. Lyakhov, and M. Valle, *Accounts of Chemical Research* **44**, 227 (2011).
- ¹¹ A. Lyakhov, A. Oganov, H. Stokes, and Q. Zhu, *Computer Physics Communications* **184**, 1172 (2013).
- ¹² J. Perdew, K. Burke, and M. Ernzerhof, *Phys. Rev. Lett.* **77**, 3865 (1996).
- ¹³ G. Kresse and J. Furthmüller, *Phys. Rev. B* **54**, 11169 (1996).
- ¹⁴ G. Kresse and D. Joubert, *Phys. Rev. B* **59**, 1758 (1999).
- ¹⁵ A. Togo, F. Oba, and I. Tanaka, *Phys. Rev. B* **78**, 134106 (2008).
- ¹⁶ P. Giannozzi, S. Baroni, N. Bonini, M. Calandra, R. Car, C. Cavazzoni, D. Ceresoli, G. Chiarotti, M. Cococcioni, I. Dabo, A. Corso, S. Gironcoli, S. Fabris, G. Fratesi, R. Gebauer, U. Gerstmann, C. Gougoussis, A. Kokalj, M. Lazzeri, L. Martin-Samos, N. Marzari, F. Mauri, R. Mazzarello, S. Paolini, A. Pasquarello, L. Paulatto, C. Sbraccia, S. Scandolo, G. Sclauzero, A. Seitsonen, A. Smogunov, P. Umari, and R. Wentzcovitch, *Journal of Physics: Condensed Matter* **21**, 395502 (2009).
- ¹⁷ A. Lyakhov and A. Oganov, *Phys. Rev. B* **84**, 092103 (2011).
- ¹⁸ X.-Q. Chen, H. Niu, D. Li, and Y. Li, *Intermetallics* **19**, 1275 (2011).
- ¹⁹ V. Mukhanov, O. Kurakevych, and V. Solozhenko, *Journal of Superhard Materials* **30**, 368 (2008).
- ²⁰ F. Murnaghan, *Proceedings of the National Academy of Sciences* **30**, 244 (1944).
- ²¹ T. Demuth, Y. Jeanvoine, J. Hafner, and J. Ángyán, *Journal of Physics: Condensed Matter* **11**, 3833 (1999).
- ²² A. Oganov, M. Gillan, and G. Price, *Phys. Rev. B* **71**, 064104 (2005).
- ²³ T. Tsuchiya, R. Caracas, and J. Tsuchiya, *Geophysical Research Letters* **31**, 1 (2004).
- ²⁴ A. Černok, E. Bykova, T. Ballaran, H.-P. Liermann, M. Hanfland, and L. Dubrovinsky, *Zeitschrift für Kristallographie — Crystalline Materials* **229**, 761 (2014).
- ²⁵ A. El Goresy, L. Dubrovinsky, T. Sharp, S. Saxena, and M. Chen, *Science* **288**, 1632 (2000).
- ²⁶ L. Dubrovinsky, N. Dubrovinskaia, S. Saxena, F. Tutti, S. Rekhi, T. Bihan, G. Shen, and J. Hu, *Chemical Physics Letters* **333**, 264 (2001).
- ²⁷ J. Zhang, Q. Zeng, A. Oganov, D. Dong, and Y. Liu, *Physics Letters A* **378**, 3549 (2014).
- ²⁸ A. Oganov and A. Lyakhov, *Journal of Superhard Materials* **32**, 143 (2010).
- ²⁹ J. Léger, J. Haines, M. Schmidt, J. Petitet, A. Pereira, and J. da Jornada, *Nature* **383**, 401 (1996).